Current Driven Domain Wall Velocities Exceeding the Spin Angular Momentum Transfer Rate in Permalloy Nanowires

Masamitsu Hayashi,[1,2] Luc Thomas,[1] Charles Rettner,[1] Rai Moriya,[1] Yaroslaw B. Bazaliy,[1] and Stuart S. P. Parkin[1,*]

[1]*IBM Almaden Research Center, San Jose, California, USA*

[2]*Department of Materials Science and Engineering, Stanford University, Stanford, California, USA*

(Received 21 August 2006; published 19 January 2007)

The velocity of domain walls driven by current in zero magnetic field is measured in permalloy nanowires using real-time resistance measurements. The domain wall velocity increases with increasing current density, reaching a maximum velocity of ~ 110 m/s when the current density in the nanowire reaches $\sim 1.5 \times 10^8$ A/cm^2. Such high current driven domain wall velocities exceed the estimated rate at which spin angular momentum is transferred to the domain wall from the flow of spin polarized conduction electrons, suggesting that other driving mechanisms, such as linear momentum transfer, need to be taken into account.

DOI: 10.1103/PhysRevLett.98.037204 PACS numbers: 85.70.Kh, 75.60.Ch, 85.75.−d

The speed at which a magnetic domain wall (DW) can travel in magnetic materials depends on the driving force, conventionally a magnetic field [1]. The field driven motion of DWs has been studied extensively in thin films [2,3] and, more recently, in magnetic nanowires [4–8]. A different method of driving DWs is to directly supply spin angular momentum to the DW by passing spin polarized current across it [7–19]. Several groups have reported current induced DW motion in nanowires formed from permalloy, but the DW velocities [16–18] they report are significantly lower, by as much as 10–100 times the maximum DW velocity allowed by the spin angular momentum transfer rate. In this Letter, we report time resolved measurements of the current driven DW velocity in permalloy nanowires. We find DW velocities of ~ 110 m/s for current densities of $\sim 1.5 \times 10^8$ A/cm^2, in the absence of any magnetic field, which exceed reasonable estimates of the spin angular momentum transfer rate.

Permalloy nanowires are made by patterning 0.5 Fe/10 AlO_x/10 $Ni_{81}Fe_{19}$/1 TaN/5 Ru (thickness in nanometers) films [20], deposited on highly resistive Si substrates. Electron-beam lithography and Ar ion etching are used to pattern both the nanowire and electrical contacts to the wire formed from 5 Ta/45 Rh. Results from a 300 nm wide nanowire are presented in detail here. 40 GHz bandwidth probes are used to make contact to the nanowire.

Figures 1(a) and 1(b) show scanning electron microscope (SEM) images of a typical nanowire together with illustrations of the resistance measurement setups. Using a suitable field sequence [7,21], a DW is created in section c_1-c_2 of the nanowire by injecting a voltage pulse into line c_1 [see Fig. 1(a) for the definitions of c_i, $i = 1, 2, 3$]. This pulse generates a local magnetic field under line c_1 sufficiently large to locally reverse the magnetization of the nanowire and thereby create a DW. A magnetic field (H) may also be applied along the wire during the pulse injection. The minimum magnitude of the voltage required to nucleate a DW is ~ 1.8 V. A fraction of the injected voltage pulse also flows into the nanowire. When a positive (negative) voltage pulse is injected into c_1, positive (negative) current flows in the nanowire from c_1 to c_2. If this current is large enough, the DW may be driven out of section c_1-c_2 through a spin-torque effect. Four experimental configurations are possible, as shown in Figs. 1(c)–1(f). The DW created in section c_1-c_2 can be either head to head (HH) or tail to tail (TT), and the current can flow in either direction across the DW. We detect the presence of a DW in the nanowire through the associated decrease in the nanowire's resistance due to the anisotropic magnetoresistance effect [21].

First, we use long voltage pulses, 100 ns long, ± 2.8 V, to study the injection of a DW into section c_1-c_2 of the nanowire. The probability P_{12} for finding a DW in this section is determined by repeating 50 times the injection procedure described above and after each injection measuring the resistance of section c_1-c_2 [Fig. 1(a)]. Black squares in Figs. 1(c)–1(f) show the probability P_{12}. For positive voltages, DWs are found in section c_1-c_2 with near certainty, for both HH and TT walls, when $|H| < 5$ Oe. Fields outside this range exceed the DW propagation field along the nanowire, so driving the DW out of this section. This is also true for negative voltages, but, in the latter case, a significant drop in P_{12} is observed close to zero field. One likely explanation is that the DW nucleated in the wire is driven out of section c_1-c_2 by the current. In order to validate this possibility, we perform a second type of measurement [Fig. 1(b)] in which we probe the probability P_{23} of finding the domain wall in section c_2-c_3. The DW comes to rest here since no current flows in this section. These experiments, shown as red circles in the graphs in Figs. 1(c)–1(f), confirm our hypothesis, as discussed in detail below.

We first consider the case when a negative voltage pulse is used to create a HH DW. Values of P_{23} close to 1 are observed near zero field, coincident with the dip in P_{12}.

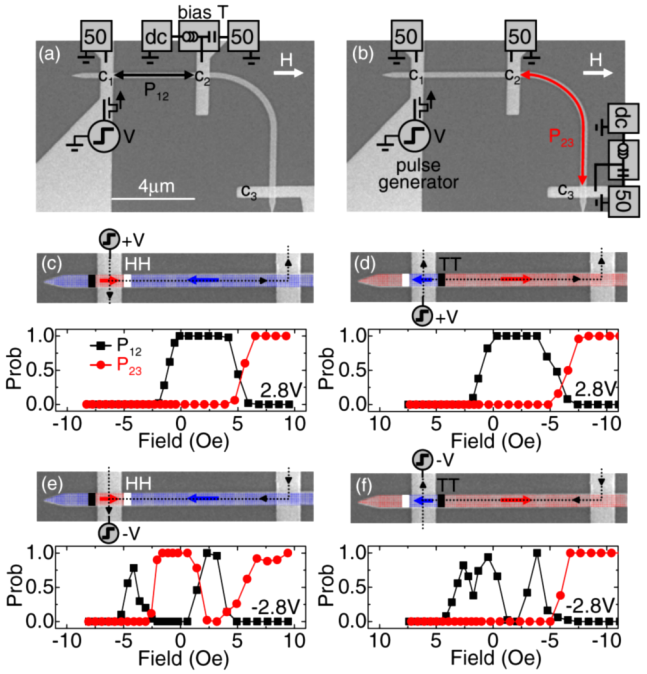

FIG. 1 (color online). (a),(b) SEM images of the device with illustrations of the measurement circuit. Labels c_1, c_2, and c_3 indicate the contact lines. The box labeled dc includes both a current source and a voltmeter connected in parallel. Solid arrows represent the portion of the permalloy nanowire across which the resistance is measured: (a) c_1-c_2 and (b) c_2-c_3. (c)–(f) Upper images: SEM images with overlays of the magnetization configuration (solid arrows) and the current path (dotted arrows). Lower panels: Probability of finding a DW in section c_1-c_2 (P_{12}, black squares) and c_2-c_3 (P_{23}, red circles), plotted as a function of the applied field. A 100 ns long voltage pulse is used in each case.

This indicates that the DW was indeed driven by current *alone* from line c_1 to section c_2-c_3. Note that the current density that flows in the nanowire when a -2.8 V pulse is applied is $\sim -1.4 \times 10^8$ A/cm^2. On the other hand, no such effect was observed for the TT DW case. As shown by the dotted lines in the upper panels in Figs. 1(c)–1(f), the current that flows from the nanowire and exits through line c_2 generates a highly localized magnetic field that can either prevent [Figs. 1(c) and 1(f)] or assist [Figs. 1(d) and 1(e)] the propagating DW to move across c_2. Thus, we infer that the TT DW is driven by the current close to line c_2 but that it is pinned to the left side of line c_2 due to this local field [22]. We estimate that this field is $\sim$40 Oe when a -2.8 V pulse is used. Note that this field is significantly smaller than the DW nucleation field. Finally, in all cases, regardless of the DW type or the voltage pulse polarity, when the magnitude of H exceeds the propagation field in the nanowire (here $\sim$5 Oe), and when the direction of H is such that it drives the DW towards section c_2-c_3 (i.e., positive H for HH and negative H for TT DWs), then P_{23} jumps from zero to one.

The measurements above, using 100 ns long pulses, clearly show that in zero field the injected DWs move ~ 4 μm under current. By determining the minimum length of the pulse required to move the DW out of section c_1-c_2, we can determine the DW velocity. When the pulse is too short, the DW remains in this section. Under these circumstances, we find two distinct values for the resistance of section c_1-c_2, as shown in the exemplary histograms of ΔR in Figs. 2(a) and 2(b) (for which two different injection pulse amplitudes of -1.8 and -2.8 V are used). ΔR is the change in resistance of section c_1-c_2 before and after injection of the voltage pulse. The two ΔR states correspond to two different DW states which we have identified from magnetic force microscopy as being transverse ($\Delta R \sim -0.23$) and vortex ($\Delta R \sim -0.3$) wall states [21]. Thus, the pulse length dependence of P_{12} can be measured for each of these DW states by identifying them from ΔR.

Figures 2(c) and 2(d) show maps of the probability P_{12} of a HH transverse [Fig. 2(c)] and vortex [Fig. 2(d)] wall remaining in section c_1-c_2 plotted as a function of the injection pulse amplitude and length. The applied field is zero, within experimental error. For illustration, line sections through the probability maps at fixed voltages of -2.0, -2.8, and -3.5 V are shown in Figs. 2(e) and 2(f). In a narrow amplitude window near the minimum

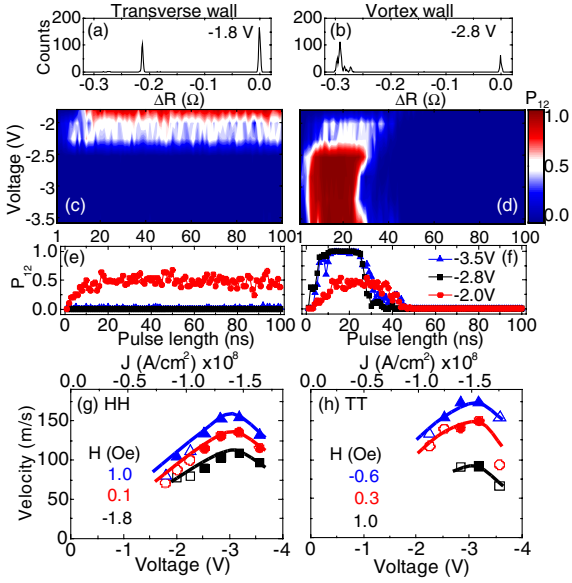

FIG. 2 (color online). (a),(b) Examples of injection of transverse and vortex DWs into section c_1-c_2 of the nanowire using -1.8 (a) and -2.8 V (b) voltage pulses (1–20 ns long), respectively. Corresponding histograms of ΔR are shown. (c),(d) Injection probability (P_{12}) maps for HH (c) transverse and (d) vortex DWs. The color scale represents the probability. The applied magnetic field is zero. (e),(f) Profiles of the probability at -2.0, -2.8, and -3.5 V for (e) transverse and (f) vortex DWs. (g),(h) Vortex DW velocities for (g) HH and (h) TT DWs plotted against the voltage pulse amplitude and the corresponding current density that flows into the nanowire. The solid (open) symbols represent data where the averaged probability of a vortex wall found in section c_1-c_2 is higher (lower) than 50%.

voltage at which a DW is nucleated (−1.8 V), a transverse DW is found in section c_1-c_2 with very high probability, independent of pulse length. For higher amplitudes, vortex DWs are found in section c_1-c_2 up to pulse lengths of ~25–30 ns, above which no DW is found. We thus surmise that the vortex DWs are driven out by sufficiently long voltage pulses.

The dependence of the vortex DW velocity on the pulse amplitude is plotted in Figs. 2(g) and 2(h) for HH and TT DWs, respectively. In each case, the velocity increases as the current density is increased to $J \sim -1.5 \times 10^8$ A/cm^2, above which a slight drop is observed. Both HH and TT DWs exhibit similar velocities, indicating that the wall motion is not significantly affected by the self fields created by the voltage pulse. Although data are not shown, we find that the DW has a transverse structure when $H \sim$ 2–4 Oe, the field range in which a DW is trapped in section c_1-c_2 for negative pulse voltages, as shown in Fig. 1(e). Two possible scenarios can be considered: either a transverse wall is nucleated and trapped, or a vortex wall is first nucleated but then is transformed into a transverse wall during its subsequent propagation and is then trapped [17].

One limitation of the quasistatic experiments is the possibility that the DW moves after the end of the current pulse, so overestimating the DW velocity. Time resolved resistance measurements are conducted to obtain a more precise measurement of the DW velocity, by replacing the dc measurement setup in Fig. 1(a) with a digital oscilloscope connected to c_2 [7]. The role of the voltage pulse injected from line c_1 is now threefold in this experiment: (i) creating the DW, (ii) injecting current into the nanowire, and (iii) supplying a signal to the oscilloscope to measure the nanowire resistance in real time. Typical signal traces are shown in Fig. 3(a), for the case of a HH DW created using a −2.8 V voltage pulse. The traces are obtained by averaging the measurement ~16 000 times in order to obtain a sufficient signal to noise ratio.

The signal ΔV is zero at $t < 0$ when no DW is in section c_1-c_2 and increases to a value A, proportional to ΔR, when it enters this section. For small and zero fields, the signal is nearly constant before decreasing, after a time τ, as defined in Fig. 3(a), to zero. At higher fields, the signal is more complex. In particular, the signal decreases during the DW's motion along the wire which might be indicative of transformations in the DW state and/or distributions in the DW's velocity. Furthermore, in an intermediate field regime the signal decreases to a nonzero value A_2 [see 4 Oe trace in Fig. 3(a)]. The amplitudes A_1 and A_2 are defined to represent, respectively, the approximate probability of a DW exiting or remaining in section c_1-c_2 of the nanowire, and thus $A = A_1 + A_2$.

A_1 and A_2 are plotted in Fig. 3(b) as a function of the applied field H. These data show that the probability of a DW exiting section c_1-c_2 is high in a narrow field range near zero field, consistent with the quasistatic results in Fig. 1(e). In addition, A_1 drops at ~4 Oe, coincident with the field range where transverse DWs are trapped. The DW

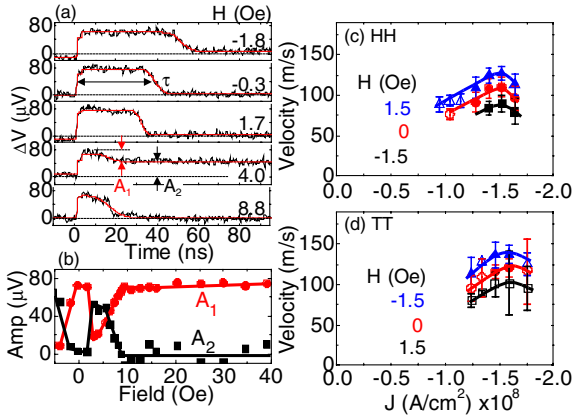

FIG. 3 (color online). (a) Typical signal traces $\Delta V(t)$ for the fields indicated in each panel. The voltage pulse is injected at $t = 0$. A voltage pulse, −2.8 V and 100 ns long, is used to inject a HH DW. The corresponding current density that flows into the permalloy nanowire is -1.4×10^8 A/cm^2. Solid red lines are fits using an error function [7]. (b) Amplitudes A_1 and A_2, defined in (a), plotted as a function of the applied field. A −2.8 V, 100 ns long voltage pulse is used to inject a HH DW. (c),(d) DW velocity near zero field plotted versus the current density. Velocities of (c) HH and (d) TT DWs are shown. The solid (open) symbols represent data where the averaged probability of a DW exiting section c_1-c_2 is higher (lower) than 50%. Error bars correspond to $\frac{\Delta\tau}{\tau}v$, where $\Delta\tau$ and v represent the fall time of $\Delta V(t)$ and the velocity, respectively.

velocity is plotted as a function of current density in Figs. 3(c) and 3(d) for HH and TT DWs, respectively, at three different fields near zero. The DW velocity is deduced by dividing the length of section c_1-c_2, ~4 μm [23], by τ. In good agreement with the quasistatic results, the DW velocity increases as the current density is increased up to $J \sim -1.5 \times 10^8$ A/cm^2, above which a slight drop is observed. A maximum DW velocity of ~110 m/sec is observed in zero field [24]. These velocities are much higher than previously reported values in permalloy nanowires [16–18]. We speculate that this discrepancy may be due to differences in the roughness of either the edges or the surfaces of the nanowires, arising from differences in the method of fabrication of the nanowire and the under- and overlayers used here to promote smooth nanowire surfaces [20]. We find no evidence that the initial state of the DW, whether it is moving or stationary, affects its velocity significantly.

A slight drop in the DW velocity is observed at the highest current density in both the quasistatic and the real-time measurements. One possible explanation for the drop may be Joule heating, although we estimate that the maximum temperature increase is only ~130 K at the highest current density. Another possible explanation is a change in the DW propagation mode analogous to the field induced Walker breakdown phenomenon, as described in Ref. [13].

To address the question as to whether the high DW velocities we observe can be accounted for by the rate of

spin momentum transfer from the current, we use the one-dimensional DW model [1,11–13]. In such a model, the time averaged DW velocity, in the absence of field, can be expressed as $v_{1D} = \frac{\beta}{\alpha} u (J \leq J^*)$ [25], where $J^* \equiv \frac{1}{2}\gamma H_K \Delta \frac{\alpha}{|\alpha-\beta|}(eM_S/\mu_B P)$, H_K is the anisotropy field, Δ is the DW width, α is the Gilbert damping constant, μ_B is the Bohr magneton, P is the current polarization, e is the electron charge, M_S is the saturation magnetization, and β is the nonadiabatic spin-torque term [11–13]. The parameter $u = \mu_B JP/eM_S$, in units of velocity, directly represents the rate of spin angular momentum transfer from the conduction electrons to the local moments.

We compare v_{exp}, the maximum DW velocity ($\sim$110 m/s) we observe at $J \sim 1.5 \times 10^8$ A/cm^2, with v_{1D} for different β. First, if $\beta < \alpha$, v_{1D} is smaller than u for any value of J and approaches u only when $J \gg J^*$. The largest possible spin momentum transfer rate u, corresponding to $J \sim 1.5 \times 10^8$ A/cm^2, is $\sim$110 m/s, when P is equal to its maximum possible value of 1. Thus, in order to match v_{1D} with v_{exp}, it follows that $J \gg J^*$ [25]. We find that $J^* \sim 2.1 \times 10^8$ A/cm^2 using values of $H_K \sim 750$ Oe and $\Delta \sim 23$ nm obtained from micromagnetic simulations for a vortex DW [26], when $\beta = 0$ (J^* is even bigger when β is nonzero). Thus, we infer that J is smaller than J^*, and therefore β cannot be smaller than α. Second, if $\beta = \alpha$, $v_{1D} = u$ for any value of J, which in turn requires $P = 1$ ($u \sim 110$ m/s) to match v_{1D} and v_{exp}, which is unrealistic. Taking a more realistic value of P ($\sim$0.4–0.9) [27–29] and considering likely inefficiency in the spin transfer process, β must therefore be larger than α to match v_{1D} and v_{exp}. This indicates that the DW is moving faster than the rate of spin angular momentum transfer, i.e., $v_{1D} = \frac{\beta}{\alpha} u$, with $\beta > \alpha$.

In summary, we have measured current driven DW velocities in permalloy nanowires, with both real-time and quasistatic techniques. DW velocities reaching $\sim$110 m/s are found for current densities of $\sim 1.5 \times 10^8$ A/cm^2 in zero magnetic field. These velocities exceed the estimated rate of spin angular momentum transfer from the conduction electrons to the local moments, indicating that some other mechanism, for example, a linear momentum transfer effect, is necessary to obtain high current driven DW velocities.

We thank DMEA for partial support of this work.

*Electronic address: parkin@almaden.ibm.com

[1] A. P. Malozemoff and J. C. Slonczewski, *Magnetic Domain Walls in Bubble Material* (Academic, New York, 1979).
[2] V. G. Bar'yakhtar *et al.*, *Dynamics of Topological Magnetic Solitons* (Springer-Verlag, Berlin, 1994).
[3] A. Hubert and R. Schafer, *Magnetic Domains: The Analysis of Magnetic Microstructures* (Springer, New York, 2001).
[4] T. Ono *et al.*, Science **284**, 468 (1999).
[5] G. S. D. Beach *et al.*, Nat. Mater. **4**, 741 (2005).
[6] D. Atkinson *et al.*, Nat. Mater. **2**, 85 (2003).
[7] M. Hayashi *et al.*, Phys. Rev. Lett. **96**, 197207 (2006).
[8] G. S. D. Beach *et al.*, Phys. Rev. Lett. **97**, 057203 (2006).
[9] L. Berger, Phys. Rev. B **73**, 014407 (2006).
[10] L. Berger, J. Appl. Phys. **55**, 1954 (1984).
[11] G. Tatara and H. Kohno, Phys. Rev. Lett. **92**, 086601 (2004).
[12] S. Zhang and Z. Li, Phys. Rev. Lett. **93**, 127204 (2004).
[13] A. Thiaville *et al.*, Europhys. Lett. **69**, 990 (2005).
[14] S. E. Barnes and S. Maekawa, Phys. Rev. Lett. **95**, 107204 (2005).
[15] C. H. Marrows, Adv. Phys. **54**, 585 (2005), and references therein.
[16] A. Yamaguchi *et al.*, Phys. Rev. Lett. **92**, 077205 (2004).
[17] M. Klaui *et al.*, Phys. Rev. Lett. **95**, 026601 (2005).
[18] M. Klaui *et al.*, Appl. Phys. Lett. **88**, 232507 (2006).
[19] M. Yamanouchi *et al.*, Phys. Rev. Lett. **96**, 096601 (2006).
[20] The film is designed to minimize any structural and magnetic roughness in the NiFe layer. The Fe/AlO_x underlayers are used to provide a smooth and clean template layer for the NiFe layer. A Ru cap layer is chosen since its oxide is conducting, so allowing for low resistance electrical contacts. TaN is used as an oxidation barrier and to prevent any adverse effects from the Ru layer on the magnetic properties of permalloy.
[21] M. Hayashi *et al.*, Phys. Rev. Lett. **97**, 207205 (2006).
[22] When a DW is located under the contact line (c_2), a reduced or zero ΔR is observed since most of the current flows through the contact line instead of the nanowire.
[23] The local field generated from the voltage pulse injected into line c_1 may aid the subsequent motion of the DW. However, we estimate that this local field is larger than the propagation field over a maximum distance of only $\sim$400 nm from the edge of line c_1 at the highest pulse voltage.
[24] Limited data on the current induced DW velocity in zero field in our previous study [7] indicated zero velocity. We speculate that this was because our experimental setup was limited to measurements of DW velocities above 50 m/s and that large field steps were used with a possible small error in the actual zero field.
[25] For $J > J^*$,

$$v_{1D} = \frac{\beta}{\alpha} u \pm \frac{\sqrt{(1 - \frac{\beta}{\alpha})^2 u^2 - (\frac{1}{2}\gamma \Delta H_K)^2}}{1 + \alpha^2},$$

with $\pm$ corresponding to $\beta < \alpha$ and $\beta > \alpha$, respectively. For all β, $v_{1D} \rightarrow u$ when $J \gg J^*$. See Ref. [13] for details.
[26] Micromagnetic simulations of the field dependence of the DW velocity are performed to obtain the Walker breakdown field H_{WB} and the DW mobility μ. Then, using the 1D model, we calculate $H_K = 2H_{WB}/\alpha$ and $\Delta = \mu\alpha/\gamma$.
[27] J. Bass and W. P. Pratt, Jr., J. Magn. Magn. Mater. **200**, 274 (1999).
[28] J. W. F. Dorleijn, Philips Res. Rep. **31**, 287 (1976).
[29] R. J. Soulen *et al.*, Science **282**, 85 (1998).